Glutathione Peroxidase-like Antioxidant Activity of Diaryl Diselenides: A Mechanistic Study

G. Mugesh,[†] Arunashree Panda,[†] Harkesh B. Singh,*[,†] Narayan S. Punekar,[‡] and Ray J. Butcher[§]

Contribution from the Department of Chemistry and the Biotechnology Centre, Indian Institute of Technology, Powai, Bombay 400 076, India, and Department of Chemistry, Howard University, Washington, D.C. 20059

Received December 21, 1999. Revised Manuscript Received October 4, 2000

Abstract: The synthesis, structure, and thiol peroxidase-like antioxidant activities of several diaryl diselenides having intramolecularly coordinating amino groups are described. The diselenides derived from enantiomerically pure *R*-(+)- and *S*-(−)-*N*,*N*-dimethyl(1-ferrocenylethyl)amine show excellent peroxidase activity. To investigate the mechanistic role of various organoselenium intermediates, a detailed in situ characterization of the intermediates has been carried out by ^{77}Se NMR spectroscopy. While most of the diselenides exert their peroxidase activity via selenol, selenenic acid, and selenenyl sulfide intermediates, the differences in the relative activities of the diselenides are due to the varying degree of intramolecular Se···N interaction. The diselenides having strong Se···N interactions are found to be inactive due to the ability of their selenenyl sulfide derivatives to enhance the reverse GPx cycle (RSeSR + H_2O_2 = RSeOH). In these cases, the nucleophilic attack of thiol takes place preferentially at selenium rather than sulfur and this reduces the formation of selenol by terminating the forward reaction. On the other hand, the diselenides having weak Se···N interactions are found to be more active due to the fast reaction of the selenenyl sulfide derivatives with thiol to produce diphenyl disulfide and the expected selenol (RSeSR + PhSH = PhSSPh + RSeH). The unsubstituted diaryl diselenides are found to be less active due to the slow reactions of these diselenides with thiol and hydrogen peroxide and also due to the instability of the intermediates. The catalytic cycles of **18** and **19** strongly resemble the mechanism by which the natural enzyme, glutathione peroxidase, catalyzes the reduction of hydroperoxides.

Introduction

Glutathione peroxidase (GPx) is a well-known selenoenzyme that functions as an antioxidant.[1] This selenoprotein catalyzes the reduction of harmful peroxides by glutathione and protects the lipid membranes and other cellular components against oxidative damage. The enzyme catalytic site includes a selenocysteine residue in which the selenium undergoes a redox cycle involving the selenol (ESeH) as the active form that reduces hydrogen peroxides and organic peroxides. The selenol is oxidized to selenenic acid (ESeOH), which reacts with reduced glutathione (GSH) to form selenenyl sulfide adduct (ESeSG). A second glutathione then regenerates the active form of the enzyme by attacking the ESeSG to form the oxidized glutathione (GSSG) (Scheme 1). Thus, in the overall process, 2 equiv of glutathione are oxidized to the disulfide and water, while the hydroperoxide is reduced to the corresponding alcohol. The crystal structure of human plasma GPx has been determined and crystallographically refined at 2.9 Å resolution.[2] In contrast to the bovine cellular enzyme where the selenium atom exists as a selenol, the selenium was found to exist as a seleninic acid [E-SeO_2H] in the crystals of human plasma GPx. This suggests that the seleninic acid ($ESeO_2H$) can also be formed in the presence of high concentrations of hydroperoxide, but it is believed to lie off the main catalytic pathway.

Scheme 1. Proposed Catalytic Mechanism of Glutathione Peroxidase

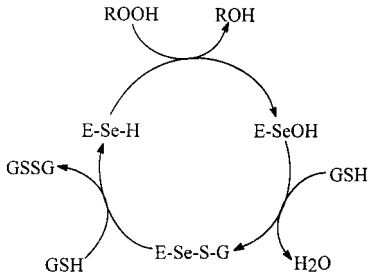

Recently, some simple organoselenium compounds have been shown to mimic the GPx activity in vitro. Among them the most promising drug was Ebselen (PZ 51, 2-phenyl-1,2-benzoisoselenazol-3-(2*H*)-one, **1**), a heterocyclic compound that functions as an antioxidant.[3] After the discovery of this exciting compound, several other mimetics have been reported which include the Ebselen analogues,[4] benzoselenazolinones,[5] selenenamide

[†] Department of Chemistry, Indian Institute of Technology.
[‡] Biotechnology Centre, Indian Institute of Technology.
[§] Howard University.

(1) (a) Flohé, L.; Loschen, G.; Günzler, W. A.; Eichele, E. *Hoppe-Seyler's Z. Physiol. Chem.* **1972**, *353*, 987. (b) *Selenium in Biology and Human Health*; Burk, R. F., Ed.; Springer-Verlag: New York, 1994 (c) Flohe, L. *Curr. Top. Cell Regul.* **1985**, *27*, 473. (d) Tappel, A. L. *Curr. Top. Cell. Regul.* **1984**, *24*, 87. (e) Epp, O.; Ladenstein, R.; Wendel, A. *Eur. J. Biochem.* **1983**, *133*, 51.

(2) Ren, B.; Huang, W.; Åkesson, B.; Ladenstein, R. *J. Mol. Biol.* **1997**, *268*, 869.

(3) (a) Müller; A.; Cadenas, E.; Graf, P.; Sies, H. *Biochem. Pharmacol.* **1984**, *33*, 3235. (b) Wendel, A.; Fausel, M.; Safayhi, H.; Tiegs, G.; Otter, R. *Biochem. Pharmacol.* **1984**, *33*, 3241. (c) Parnham, M. J.; Kindt, S. *Biochem. Pharmacol.* **1984**, *33*, 3247. (d) Wendel, A. European Patent 0,-165,534, 1985.

10.1021/ja994467p CCC: $20.00
Published on Web 01/13/2001

(**2**)[6a] and related derivatives,[6b] diaryl diselenides,[7] various tellurides and ditellurides,[8] and the semisynthetic enzyme selenosubtilisin.[9] The diaryl diselenides (**3**, **4**, **5**) with basic amino groups have attracted much attention as GPx mimics because the Se···N intramolecular nonbonded interactions (i) activate the Se−Se bond toward the oxidative cleavage, (ii) stabilize the resulting selenenic acid intermediate against further oxidation, and (iii) enhance the nucleophilic attack of the thiol at the sulfur rather than selenium compared with unsubstituted phenylselenyl sulfide.[7] Hilvert et al. have also reported that a basic histidine residue at the active center of selenosubtilisin facilitates the reduction of selenenyl sulfide to selenolate with thiols.[10] In GPx, Gln79 and Trp153 may play such a role, as these are located within hydrogen-bonding distances to the selenium atom [Cso45 Se···N(Gln79) 3.5 Å; Cso45 Se···N(Trp153) 3.6 Å].[2] More recently, a new class of diselenides containing an oxygen atom in close proximity to selenium (**6**−**11**) have been reported as GPx mimics.[11] Although the Se···O interactions were shown to increase the catalytic activity, diselenide **10** in which the Se···O interactions are expected to be strong has exhibited only 50% of the activity of compound **6**. Compound **11** containing an electron-donating substituent (methoxy group) in the para-position showed the highest activity of the series.

In continuation of our work on intramolecularly coordinated organochalcogens,[12] we reported, in a preliminary communication, the GPx activity of a series of diaryl diselenides having intramolecular Se···N interactions. It was found that the diselenides (**20**−**22**) which have quite strong Se···N intramolecular interactions were less active whereas the diselenides (**18**, **19**) which have a built-in coordinating basic amino group but did not have Se···N interactions showed excellent GPx activity.[13] Although the large difference in the activities of **18** and **19** as compared with **3** was ascribed to the presence of both the redox-active group and the amino nitrogen, the actual role of the nitrogen atom in these compounds could not be delineated from the kinetic data. It was also not clear why the diselenides which have strong Se···N interactions were inactive in the catalytic process. It is, therefore, still a matter of debate whether and to what extent the Se···N interactions contribute to the GPx activity. To this end, we have undertaken a detailed mechanistic study to investigate the role of amino groups in the catalytic cycle of diselenides. In this article, we describe the use of ^{77}Se NMR spectroscopy to identify the intermediates involved in the catalytic cycle and the role of amino groups in the activation of intermediates in addition to the detailed synthesis, structure, and kinetic studies of the diselenides. We also attempt to delineate the basic difference in the mechanism by which the amino-substituted diselenides catalyze the reduction of peroxides.

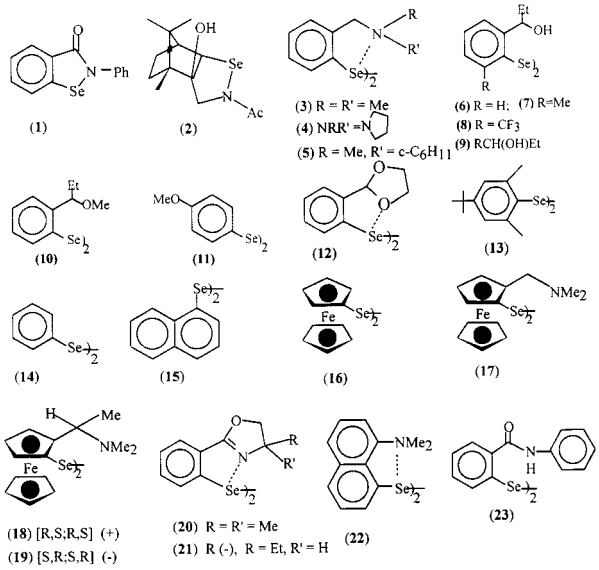

Results and Discussion

Synthesis. Diselenides **3**,[12b] **18**,[14] **19**,[14] and **23**[15] used in the present study were prepared according to literature methods. Diselenide **12** was synthesized from *o*-bromobenzaldehyde. The reaction of *o*-bromobenzaldehyde with ethylene glycol afforded the protected *o*-bromobenzaldehyde acetal (**24**). Ortho lithiation followed by selenium insertion and then oxidative workup gave a yellowish viscous liquid from which pale yellow solid **12** was obtained upon cooling (Scheme 2). The synthesis of compound **13** was first approached by the organolithium route. Addition of n-BuLi to an ethereal solution of 2-bromo-5-*tert*-butyl-*m*-xylene (**26**)[16] produced a white precipitate of the lithiated compound. Since all attempts for the insertion of Se into the C−Li bond were unsuccessful, we decided to synthesize the desired compound by the Grignard route. Reaction of **26** with magnesium turnings produced arylmagnesium bromide (**27**). Addition of selenium powder followed by oxidation afforded the desired diselenide **13** as an orange solid in good yield. Dinaphthyl diselenide **15** was synthesized from commercially

(4) (a) Jacquemin, P. V.; Christiaens, L. E.; Renson, M. J.; Evers, M. J.; Dereu, N. *Tetrahedron Lett*. **1992**, *33*, 3863. (b) Chaudie're, J.; Yadan, J.-C.; Erdelmeier, I.; Tailhan-Lomont, C.; Moutet, M. In *Oxidative Processes and Antioxidants*; Paoletti, R., Ed.; Raven Press: New York, 1994; p 165. (c) Chaudie're J.; Moutet, M.; d'Alessio, P. C. R. *Soc. Biol*. **1995**, *189*, 861. (d) Sies, H. *Free Radicals Biol. Med.* **1993**, *14*, 313.

(5) Galet, V.; Bernier, J.-L.; Hénichart, J.-P.; Lesieur, D.; Abadie, C.; Rochette, L.; Lindenbaum, A.; Chalas, J.; Renaud de la Faverie, J.-F.; Pfeiffer, B.; Renard, P. *J. Med. Chem*. **1994**, *37*, 2903.

(6) (a) Back, T. G.; Dyck, B. P. *J. Am. Chem. Soc*. **1997**, *119*, 2079. (b) Reich, H. J.; Jasperse, C. P. *J. Am. Chem. Soc.* **1987**, *109*, 5549.

(7) (a) Wilson, S. R.; Zucker, P. A.; Huang, R.-R. C.; Spector, A. *J. Am. Chem. Soc*. **1989**, *111*, 5936. (b) Iwaoka, M.; Tomoda, S. *J. Am. Chem. Soc*. **1994**, *116*, 2557. (c) Spector, A.; Wilson, S. R.; Zucker, P. A. U.S. Patent 5,321,138 (C1.546−224; C07C37/02) 1994; *Chem. Abstr*. **1994**, *121*, P 256039r. (d) Iwaoka, M.; Tomoda, S. *J. Am. Chem. Soc*. **1996**, *118*, 8077. (e) Welter, A.; Fisher, H.; Christiaens, L.; Wendel, A.; Etschenberg, E.; Dereu, N.; Kuhl, P.; Graf, E. European Patent Application EP 198277B1, 1989; *Chem. Abstr*. **1987**, *106*(05), 032613A; *Chem. Abstr*. **1987**, *106*(11), 084181C. (f) Spector, A.; Wilson, S. R.; Zucker, P. A.; Huang, R. R.; Raghavan, P. R. *Lens Eye Tox. Res*. **1989**, 773.

(8) (a) Engman, L.; Stern, D.; Cotgreave, I. A.; Andersson, C. M. *J. Am. Chem. Soc*. **1992**, *114*, 9737. (b) Engman, L.; Stern, D.; Pelcman, M.; Andersson, C. M. *J. Org. Chem*. **1994**, *59*, 1973. (c) Vessman, K.; Ekstörm, M.; Berglund, M.; Andersson, C. M.; Engman, L. *J. Org. Chem*. **1995**, *60*, 4461.

(9) (a) Wu, Z.-P.; Hilvert, D. *J. Am. Chem. Soc*. **1989**, *111*, 4513. (b) Wu, Z.-P.; Hilvert, D. *J. Am. Chem. Soc*. **1990**, *112*, 5647.

(10) (a) Bell, I. M.; Fisher, M. L.; Wu, Z.-P.; Hilvert, D. *Biochemistry* **1993**, *32*, 3754. (b) Bell, I. M.; Hilvert, D. *Biochemistry* **1993**, *32*, 13969.

(11) Wirth, T. *Molecules* **1998**, *3*, 164.

(12) (a) Kaur, R.; Singh, H. B.; Butcher, R. J. *Organometallics* **1995**, *14*, 4755. (b) Kaur, R.; Singh, H. B.; Patel, R. P. *J. Chem. Soc., Dalton Trans.* **1996**, 2719. (c) Menon, S. C.; Singh, H. B.; Patel, R. P.; Das, K.; Butcher, R. J. *Organometallics* **1997**, *18*, 563. (d) Mugesh, G.; Singh, H. B.; Patel, R. P.; Butcher, R. J. *Inorg. Chem.* **1998**, *37*, 2663. (e) Panda, A.; Mugesh, G.; Singh, H. B.; Butcher, R. J. *Organometallics* **1999**, *18*, 1986. (f) Mugesh, G.; Singh, H. B.; Butcher, R. J. *Tetrahedron: Asymmetry* **1999**, *10*, 237. (g) Mugesh, G.; Panda, A.; Singh, H. B.; Butcher, R. J. *Chem. Eur. J*. **1999**, *5*, 1411. (h) Mugesh, G.; Singh, H. B.; Butcher, R. J. *Eur. J. Inorg. Chem.* **1999**, 1229. (i). Mugesh, G.; Singh, H. B.; Butcher, R. J. *J. Organomet. Chem.* **1999**, *577*, 243.

(13) Mugesh, G.; Panda, A.; Singh, H. B.; Punekar, N. S.; Butcher, R. J. *Chem. Commun.* **1998**, 2227.

(14) (a) Nishibayashi, Y.; Singh, J. D.; Uemura, S.; Fukuzawa, S. *Tetrahedron Lett.* **1994**, *35*, 3115. (b) Nishibayashi, Y.; Singh, J. D.; Uemura, S.; Fukuzawa, S. *J. Org. Chem*. **1995**, *60*, 4114.

(15) Engman, L.; Hallberg, A. *J. Org. Chem.* **1989**, *54*, 2964.

(16) Tashiro, M.; Yamato, T. *J. Chem. Soc., Perkin Trans. 1* **1979**, 176.

Scheme 2. Synthetic Routes to the Syntheses of Diselenides **12**, **13**, and **20**−**22**

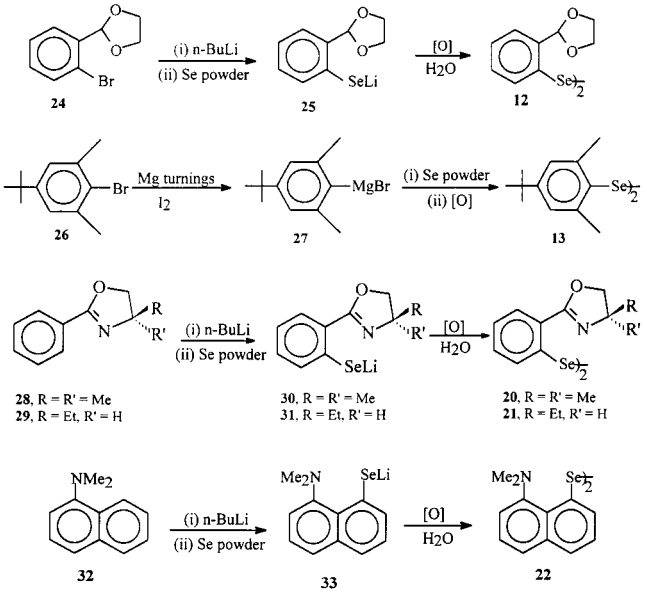

available 1-bromonaphthalene by the Grignard route. Compounds **16** and **17** were synthesized according to literature methods with minor modifications.[17,18] Monolithiation of ferrocene was achieved by the addition of t-BuLi to a solution of ferrocene in THF at 0 °C which was further reacted with finely ground selenium to give the lithium areneselenolate. Oxidative workup of the lithium areneselenolate then gave the diferrocenyl diselenide (**17**) in moderate yield. Monolithiation of *N*,*N*-dimethylaminomethylferrocene with n-BuLi in ether followed by selenium insertion and oxidative workup afforded **17**. Heteroatom-directed lithiation of 4,4-dimethyl-2-phenyloxazoline (**28**), *R*-(−)-4-ethyl-2-phenyloxazoline (**29**), and 8-(*N*,*N*-dimethylamino)-1-naphthalene (**32**) with n-BuLi followed by selenium insertion and oxidative workup afforded **20**, **21**, and **22**, respectively.[13]

Catalytic Activity. The catalytic activity was studied according to the method reported by Tomoda et al.[7b] using benzenethiol (PhSH) as a glutathione alternative. The initial rates (v_0) for the reduction of H_2O_2 (3.75 mM) by thiol (1 mM) in the presence of various catalysts (0.01 mM) (eq 1) were determined in methanol medium by monitoring the UV absorption at 305 nm due to the formation of diphenyl disulfide (PhSSPh).

$$H_2O_2 + 2PhSH \xrightarrow{\text{catalyst}} 2H_2O + PhSSPh \qquad (1)$$

The relative activities of the compounds are summarized in Table 1. The uncatalyzed reduction rate was very slow (entry **a**, $v_0 = 0.15 \pm 0.04\ \mu M{\cdot}min^{-1}$), but a considerable enhancement in the rate was observed when the simple diselenide **14** was added (entry **d**, $v_0 = 0.55 \pm 0.18\ \mu M{\cdot}min^{-1}$). There was no noticeable effect on the reduction rate when only ferrocene was used as catalyst. However, *N*,*N*-dimethyl(ferrocenylethyl)amine, a ferrocene compound containing the basic amino group, showed a much better activity (entry **e**, $v_0 = 3.16 \pm 0.52\ \mu M{\cdot}min^{-1}$). Although there was a slight enhancement in the rate by the addition of *N*,*N*-dimethyl(ferrocenylethyl)amine along with **14** (entry **f**, $v_0 = 3.83 \pm 0.32\ \mu M{\cdot}min^{-1}$), the cooperative effects of selenium and the basic amino nitrogen did not enhance the rate since the relative initial reduction rate of the mixed case was almost equal to the sum of those in the individual cases ($3.71 \pm 0.70\ \mu M{\cdot}min^{-1}$). There was a significant improvement in the activity when the phenyl groups in **14** were replaced by a redox active ferrocenyl group, **16** (entry **h**, $v_0 = 3.39 \pm 0.37\ \mu M{\cdot}min^{-1}$). As expected, the rate observed by the addition of *N*,*N*-dimethyl(ferrocenylethyl)amine to **16** (entry **i**, $5.78 \pm 0.79\ \mu M{\cdot}min^{-1}$) was almost equal to the sum of their rates in the individual cases ($6.55 \pm 0.45\ \mu M{\cdot}min^{-1}$). However, the amino-substituted diferrocenyl diselenide (**17**) showed much better activity (entry **j**, $36.10 \pm 0.12\ \mu M{\cdot}min^{-1}$).

Table 1. Initial Reduction Rates (v_0)[a] of H_2O_2 (3.75 mM) with PhSH (1 mM) in Methanol (solvent) in the Presence of Various Selenium Catalysts (0.01 mM)

entry	catalyst	v_0,[b] $\mu M{\cdot}min^{-1}$
a	none	0.15(0.04)
b	**12**	5.84(0.15)
c	**13**	inactive
d	**14**	0.55(0.18)
e	*S*(−) amine[c]	3.16(0.52)
f	**14** + *S*(−) amine	3.83(0.32)
g	**15**	5.32(0.58)
h	**16**	3.39(0.37)
i	**16** + *S*(−) amine	5.78(0.79)
j	**17**	36.10 (0.12)
k	**3**	28.38(3.88)
l	**18**	574.01(23.98)
m	**19**	466.49(28.26)
n	**20**	inactive
o	**21**	inactive
p	**22**	inactive
q	**23**	0.35(0.09)

[a] Obtained by Lineweaver−Burk plots. [b] Standard deviations are shown in parentheses. [c] *S*-(−)-*N*,*N*-Dimethyl(ferrocenylethyl)amine.

The initial rate in the presence of crystalline Wilson's catalyst (**3**), which has been previously used as a liquid or HCl salt,[7a] was $28.38 \pm 3.88\ \mu M{\cdot}min^{-1}$ (entry **k**). Surprisingly, under similar conditions, the initial rates for diselenides **18** and **19** were 574.01 ± 23.98 (entry **l**) and 466.49 ± 28.26 (entry **m**) $\mu M{\cdot}min^{-1}$, respectively. Diselenides **20**, **21**, and **22** in which the Se···N interactions are very strong did not show any noticeable activity by this method. Compound **13**, which has a strong electron-donating substituent in the para position, was also found to be inactive even when a 10-fold excess amount of the catalyst was used (entry **c**). This is in agreement with the report of Wirth[11] and Engman et al.[8] that all bis *ortho*-substituted diselenides are less active. The activity of compound **12**, which exhibits Se···O nonbonded interactions [Se(1A)···O(1A) 3.006 Å; Se(1B)···O(1B) 2.940 Å] in the solid state, was almost equal to that of **15**. Diselenide **23**, which was shown to be more active than Ebselen,[7e] was found to be less active than other diselenides. The low activity of **23** is probably due to the fact that the presence of a secondary amino group in the ortho position leads to the formation of a cyclic selenenamide and then a stable selenenyl sulfide, which in turn reacts with thiol very slowly to give the disulfide.[3c]

A dramatic increase in the initial reduction rate of **18** and **19** compared with other catalysts may be ascribed to the synergistic effect of amino substituents and the redox-active ferrocenyl groups. While compound **16** is much more reactive than **14**, the observation that **16**, which also has the redox-active ferrocenyl group, is much less reactive than **18** and **19** clearly suggests that the nearby nitrogen moiety should be responsible for the activity enhancement of **18** and **19** in the present redox system. On the other hand, although compounds **17**, **18**, and

(17) Herberhold, M.; Leitner, P. *J. Organomet. Chem.* **1987**, *336*, 153.
(18) Gornitzka, H.; Besser, S.; Herbts-Irmer, R.; Kilimann, U.; Edelmann, F. T. *J. Organomet. Chem.* **1992**, *437*, 299.

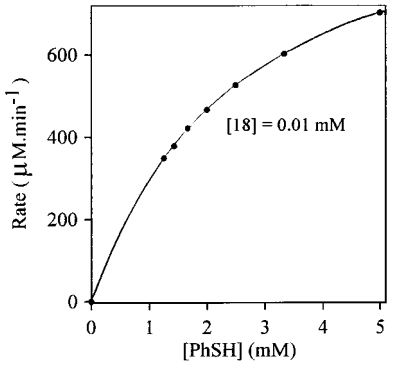

Figure 1. A representative plot of initial rates (v_0) at different concentrations of the substrate and at 0.01 mM of catalyst **18**. The initial H_2O_2 concentration was fixed at 3.75 mM.

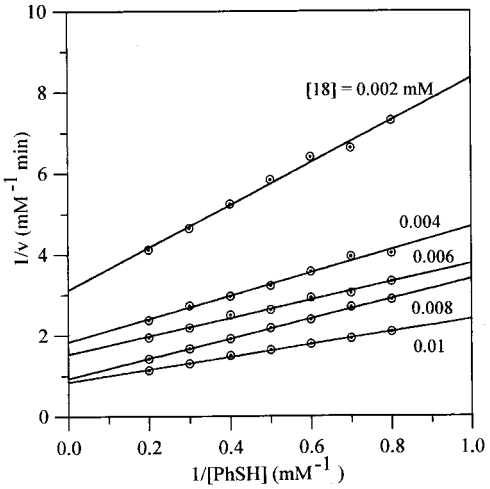

Figure 2. Lineweaver−Burk plots obtained for the model reaction in the presence of 0.002−0.01 mM of **18**. The initial H_2O_2 concentration was fixed to 3.75 mM.

19 have similar amino groups and ferrocenyl units, the large increase in the activities of **18** and **19** as compared with **17** indicates that the stabilizing interactions between selenium and the nitrogen atom may differ during the catalytic process.

Kinetics. To probe the mechanism by which diselenides **18** and **19** promote the peroxidase reaction, detailed kinetic studies were undertaken. The plot of initial rates against the catalytic concentration gave a straight line, which indicated that the peroxidase activity is linearly proportional to the concentration of catalysts. When the concentration of catalyst (**18**) was maintained constant while substrate concentration [PhSH] was increased, a rapid increase of rate was observed in the initial stages; however, when the substrate concentration was increased further, the rate became constant (Figure 1). At the same time, when the concentration of catalyst was increased, the rates become very high for higher concentrations of PhSH. From this observation it is clear that the catalyst−substrate complex (RSeSPh) does certainly exist during the catalytic cycle, which is similar to the one shown in Scheme 1 where the rate depends on the concentration of ESeSG. Double-reciprocal plots (Lineweaver−Burk plots) of initial rate vs substrate concentration yielded families of linear lines (Figures 2 and 3). The parallel lines correspond to different concentrations of the catalyst and indicate that the rates increase linearly with the concentration of the catalyst. The apparent kinetic parameters obtained at several PhSH and H_2O_2 concentrations are summarized in Table 2. It is worth noting that the Michaelis constant (K_m) values for **18** (1.81 ± 0.10 mM) and **19** (1.93 ± 0.09 mM) were much

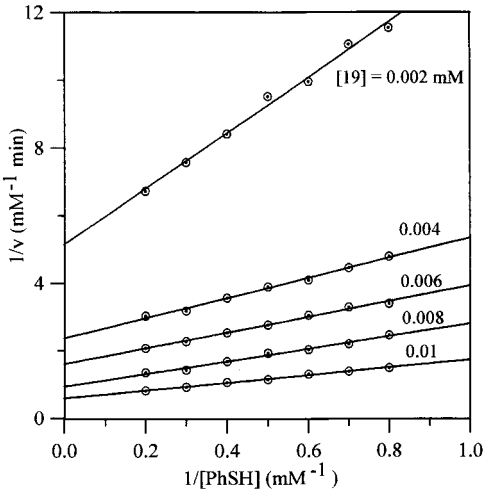

Figure 3. Lineweaver−Burk plots obtained for the model reaction in the presence of 0.002−0.01 mM of **19**. The initial H_2O_2 concentration was fixed to 3.75 mM.

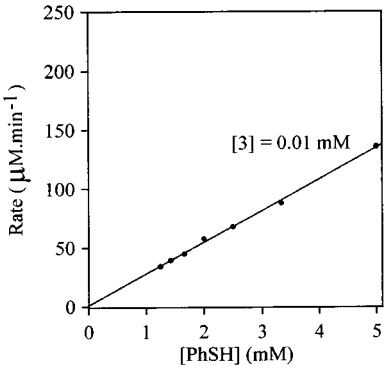

Figure 4. Plot of initial rates (v_0) at 0.01 mM of catalyst **3** against the substrate concentration. The initial H_2O_2 concentration was fixed to 3.75 mM.

lower than those for **3** (28.91 ± 0.03 mM) under similar conditions, thus indicating a much stronger affinity of the catalysts (**18** and **19**) for the substrate. From the k_{cat} (117.23 ± 2.45 min^{-1} for **18** and 169.85 ± 1.38 min^{-1} for **19**) and K_m values, the catalytic efficiencies (η) of **18** and **19** were determined to be 64.70 ± 0.95 and 87.87 ± 0.75 mM^{-1} min^{-1}, respectively, whereas the catalytic efficiency for **3** was only 2.98 ± 0.07 mM^{-1} min^{-1}. Moreover, in contrast to the behavior of **18** and **19** which showed saturation kinetics at higher concentrations of PhSH (Figure 1), saturation kinetics was not observed for **3** (Figure 4). This indicates that the rate becomes maximum for **3** only at higher concentrations of PhSH compared with H_2O_2. In other words, the reaction proceeds forward (eq 2) only when the concentration of PhSH exceeds the concentration of H_2O_2. At a lower concentration of thiol, the backward reaction may become more favorable than the forward reaction. This assumption is indeed proved by ^{77}Se NMR experiments (vide infra).

$$\mathrm{RSeOH} \underset{\mathrm{H_2O_2}}{\overset{\mathrm{PhSH}}{\rightleftharpoons}} \mathrm{RSeSPh} \xrightarrow{\mathrm{PhSH}} \mathrm{RSeH} + \mathrm{PhSSPh} \qquad (2)$$

Mechanism. To know the detailed mechanism of the peroxidase reaction we next set out to use ^{77}Se NMR spectroscopy since ^{77}Se is a very sensitive NMR nucleus and it is easily influenced by its chemical environment. Moreover, all three major intermediates, i.e., RSeH, RSeOH, and RSeSPh, are expected to show large differences in their chemical shift values. Compounds **18** and **20** were chosen to investigate the basic

Table 2. The Maximum Velocity (V_{max}), Michaelis Constant (K_m), Catalytic Constant (k_{cat}), and Catalytic Efficiency (η) for Catalysts **18** and **19** at Different Concentrations

		V_{max} (mM·min^{-1})		K_m (mM)		k_{cat} (min^{-1})		η (mM^{-1}·min^{-1})	
entry	[**18**] and [**19**] (mM)	**18**	**19**	**18**	**19**	**18**	**19**	**18**	**19**
a	0.001	0.044	0.049	1.03	1.38	44.30	48.60	42.97	35.17
b	0.002	0.320	0.194	1.67	1.59	160.04	97.02	95.61	60.94
c	0.004	0.543	0.422	1.54	1.26	135.73	105.61	87.97	84.01
d	0.006	0.651	0.623	1.45	1.44	108.50	103.77	74.67	71.91
e	0.008	1.066	1.069	2.61	1.99	133.15	133.61	50.94	67.24
f	0.010	1.172	1.699	1.81	1.93	117.23	169.85	64.70	87.87

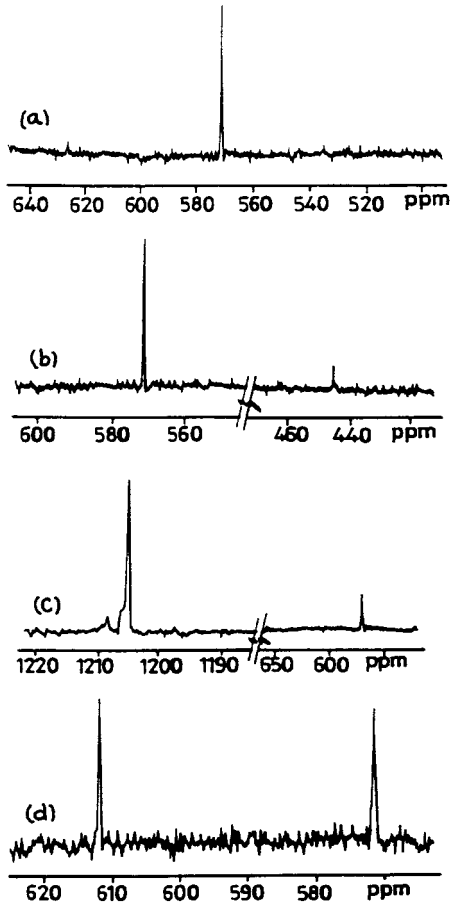

Figure 5. Room temperature ^{77}Se NMR spectra in 1:1 $CDCl_3$:CH_3-OH: (a) isolated **35**, (b) a 1:4 mixture of **35** and PhSH, (c) a 1:1 mixture of **35** and H_2O_2, and (d) a 1:1 mixture of **35** and 4-methoxybenzenethiol.

difference between the activities of the diselenides. Compound **20** belongs to the category of less active compounds which has very strong Se···N interaction whereas compound **18** belongs to the category of more active compounds in which there is no Se···N interaction. Reactions were followed by ^{77}Se NMR for 0−10 min. The signals, generally, appeared within a minute and did not change positions with passage of time.

Reactions of Diselenide 20 with Thiol and Peroxide. From the time of appearance of the ^{77}Se NMR signals, the reaction of **20** (δ 449.2 ppm) with PhSH was found to be extremely fast. Reaction of **20** with an excess of PhSH afforded the expected selenenyl sulfide **35** (574.5 ppm) whose ^{77}Se NMR chemical shift position was confirmed by its independent synthesis (Figure 5a). The signal of **35** shifted downfield by 48.5 ppm from that of PhSeSPh (526.0 ppm),[19] strongly suggesting the existence of Se···N nonbonded interaction. A similar interaction has been observed by Tomoda et al. in the selenenyl sulfide derived from **5** (δ 571.9 ppm).[7b] In this particular case, the strength of the Se···N interaction was evaluated to be 73.2 ± 4.5 kJ/mol by variable-temperature ^{1}H NMR spectroscopy. The relatively stronger Se···N interaction in **35** is probably due to the rigidity of the oxazoline ring which is involved in π-conjugation with the phenyl ring. In agreement with this, a recent report by Tomoda et al. has shown that the Se···O interaction in 2-formylbenzeneselenenyl sulfide is much stronger than that of 2-hydroxymethylbenzene selenenyl sulfide due to π-conjugation between the formyl group and the phenyl ring in the former derivative.[20] When diselenide **20** was treated with 1 equiv of PhSH, we were unable to detect the appearance of any signal expected for the selenol (**34**). An authentic sample of **34** (^{77}Se NMR δ 9.9 ppm; J_{Se-H} = 20.3 Hz) was prepared for comparison by reduction of **20** with sodium borohydride, followed by acidification with dilute HCl. The chemical shift of **34** is close to the value reported for the selenol derived from **5** (δ 22 ppm).[7b] Although **34** was not observed from the reaction of **20** with PhSH, we postulate that the selenol formed during this process may get readily oxidized to the diselenide in the presence of air as evidenced by a strong signal at 449.2 ppm for the diselenide. However, a large upfield shift in the signal of selenol compared with the chemical shift of PhSeH (145.0 ppm)[21] further indicates the presence of significant negative charge on the selenium atom.

When an equimolar amount of H_2O_2 was added immediately after the addition of PhSH to the diselenide, a new signal was observed at 1206.1 ppm, which corresponds to the selenenic acid **36**. This suggests that the oxidation of selenol with H_2O_2 initially leads to the formation of selenenic acid. Since the formation of seleninic acid (**37**) and selenonic acid (**38**) intermediates is also possible at a higher concentration of H_2O_2, the direct observation of these products was undertaken starting from diselenide **20**. When **20** was treated with an equimolar amount of aqueous H_2O_2, a single absorption peak due to **36** was observed at 1206.1 ppm. However, when an excess amount of H_2O_2 (4 equivalent) was added to the solution, initially the peak due to **36** appeared followed by two additional signals at 1149.1 and 1138.9 ppm probably due to the formation of other more oxidized products such as seleninic acid (**37**) and selenonic acid (**38**), respectively. The ^{77}Se NMR chemical shift of **36** is

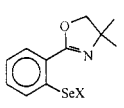

34, X = H; **35**, X = SPh
36, X = OH; **37**, X = O_2H
38, X = O_3H; **39**, X = OSPh

significantly downfield shifted compared with that of *o*-nitrobenzeneselenenic acid (1066 ppm)[22] and is close to the value reported for the selenenic acid derived from **5** (1173 ppm)[7b] thus indicating a strong Se···N interaction. Addition of

(19) Luthra, N. P.; Dunlap, R. B.; Odom, J. D. *J. Magn. Reson.* **1982**, *46*, 152.

(20) Komatsu, H.; Iwaoka, M.; Tomoda, S. *Chem. Commun.* **1999**, 205.

(21) McFarlane, W.; Wood, R. J. *J. Chem. Soc. A* **1972**, 1397.

(22) Reich, H. J.; Willis, W. W.; Wollowitz, S. *Tetrahedron Lett.* **1982**, *23*, 3319.

Scheme 3

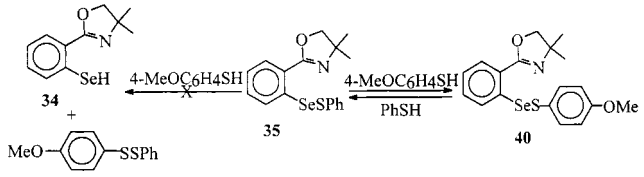

PhSH (1 equiv) to the mixture containing **36** and other oxidized products produced two new signals at 573.2 and 587.5 ppm. The signal at 573.2 ppm certainly can be assigned to **35**, which formed from the reaction of **36** with PhSH according to the normal catalytic cycle outlined in Scheme 1. The signal at 587.5 ppm ,which is shifted downfield by 15 ppm compared with that of **35**, indicates the possibility of a reaction of PhSH with other oxidized products such as **37** and **38**. Since the signal due to seleninic acid (**37**) at 1149.1 ppm disappeared completely upon thiol addition, we suggest a seleninic acid thiol ester, **39**, as an intermediate in the reaction of **37** with PhSH. The formation of seleninic acid thiol ester is consistent with the report of Engman et al. that the oxidative activation of selenosulfide with H_2O_2 affords the thiol ester as primary oxidized product.[8] The reaction of **37** with PhSH is analogous to the observation of Kice et al. that benzeneseleninic acid reacts rapidly with 3 equiv of thiol to give corresponding selenenyl sulfide (PhSeSR) and disulfide (RSSR) under a variety of conditions.[23] The addition of H_2O_2 to the mixture containing **20** and **35** produced a intense signal for **36** with a considerable decrease in the intensity of the signal observed for **35**. The signals of **20** and **35** disappeared completely when an excess of H_2O_2 was added. This indicates that both these compounds react with H_2O_2 to produce the selenenic acid **36**.

The addition of an excess of PhSH to the diselenide **20** did not give any signal for the selenol, which indicates that the selenenyl sulfide (**35**) formed during the reaction is relatively stable and is inactive toward further reaction with PhSH. The inability of **35** to produce selenol (**34**) by reaction with PhSH has also been confirmed from the reaction of isolated **35** with PhSH. When pure **35** was treated with 1 equiv of PhSH under identical experimental conditions, no signal was detected for the selenol or diselenide. A signal at 445.7 ppm for the diselenide was detected in very low intensity when the reaction mixture was kept for a long time with an excess of PhSH (Figure 5b). Importantly, when **35** was treated with an equimolar amount of H_2O_2, the signal due to **35** disappeared almost completely and a new signal at 1204.9 ppm due to the selenenic acid **36** was observed (Figure 5c). Although **35** is formed during the catalytic cycle, it goes back to the selenenic acid state (**36**) when excess H_2O_2 is present (reverse GPx cycle). This clearly indicates that the strong Se···N interaction in **35** increases the electrophilic reactivity of the selenium, which enhances a nucleophilic attack of OH^- at selenium instead of the nucleophilic attack of PhS^- at sulfur.[7d] To prove this hypothesis, a crossover experiment was carried out in which pure **35** was treated with 4-methoxybenzenethiol under identical experimental conditions (Scheme 3). The ^{77}Se NMR spectrum of the reaction mixture showed a signal at 611.8 ppm, which corresponds to a new selenenyl sulfide, **40** (Figure 5d). The reaction of diselenide with 4-methoxybenzenethiol provided the authentic sample of **40** for comparison. Although thiol interchange is taking place by the addition of 4-methoxybenzenethiol to **35** with displacement of PhSH, no conclusions can be drawn as to whether the nucleophilic attack by thiol is facile at S or Se, since redox

(23) Kice, J. L.; Lee, T. W. J. *J. Am. Chem. Soc.* **1978**, *100*, 5094.

Scheme 4

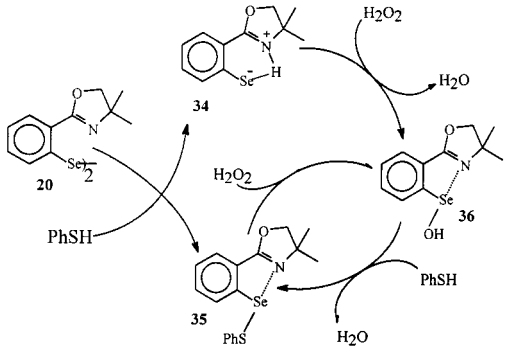

reactions at Se are normally rapid. However, from the thiol interchange and fast backward reactions of **35** and **40** with H_2O_2, we postulate that the conversion of selenenic acid to selenenyl sulfide is a reversible process. This hypothesis was further proved by UV spectroscopy by following the absorbance at 305 nm due to the formation of PhSSPh. When pure **35** was treated with 1 equiv of PhSH, there was no increase in the absorbance. The reaction mixture gave an UV spectrum that was identical with the spectrum of pure **35**. In contrast, the addition of H_2O_2 to **35** produced a new absorption band, which indicates that the reaction of **35** with H_2O_2 is the favored process.

On the basis of these experiments, we propose the following mechanism for the reduction of H_2O_2 with PhSH in the presence of **20**. The initial step is the reaction of **20** with PhSH to produce the selenol (**34**) and selenenyl sulfide (**35**). The oxidation of **34** by H_2O_2 produces the selenenic acid (**36**), which in turn reacts rapidly with PhSH to produce **35**. Compound **35** thus formed reacts rapidly, due to the presence of strong Se···N interaction with H_2O_2 to regenerate **36** (Scheme 4). The catalytic cycle is therefore completely different from the one shown in Scheme 1.

Reactions of Diselenide 18 with Thiol and Peroxide. After proving the mechanism of diselenide **20**, we subsequently proceeded to study the catalytic mechanism of more active compound **18**. All ^{77}Se NMR experiments were repeated for **18** under identical conditions. The 1:1 molar reaction of **18** (453 ppm) with PhSH produced the expected selenenyl sulfide (**42**), but the signal due to selenol (**41**) was not observed, probably due to its oxidation to **18** in the presence of air. However, when a second equivalent of PhSH was added, a complete conversion of the selenenyl sulfide to the selenol (−169.0 ppm, J_{Se-H} = 29.3 Hz) was observed. A drastic upfield shift compared with the chemical shift of benzeneselenol (145 ppm) and with that of **34** strongly suggests that the selenol is mostly dissociated in solution. The selenenyl sulfide is, therefore, reduced to selenolate (RSe^-), as its chemical shift agrees well with that reported for deprotonated selenocysteamine (−212 ppm, pH 7.1),[24] reduced selenosubtilisin (−215 ppm, pH 7.0),[25] and reduced and denatured GPx (−212 ppm, pH 8).[26] As in the case of selenosubtilisin, we presume that the increased stabilization of the selenolate is a result of interactions with the *o*-amino substituent. It must be noted that in contrast to **35**, there is no Se···N interaction in **42** as evidenced by a large upfield shift in the ^{77}Se NMR (469.1 ppm) compared with that of **35** (574.5 ppm). Attempts to isolate selenol **41** led to the oxidation of this species to the corresponding diselenide (**18**).

(24) Odom, J. D.; Dawson, W. H.; Ellis, P. D. *J. Am. Chem. Soc.* **1979**, *101*, 5815.

(25) House, K. L.; Dunlap, R. B.; Odom, J. D.; Wu, Z.-P.; Hilvert, D. *J. Am. Chem. Soc.* **1992**, *114*, 8573.

(26) Gettins, P.; Crews, B. C. *J. Biol. Chem.* **1991**, *266*, 4804.

Scheme 5

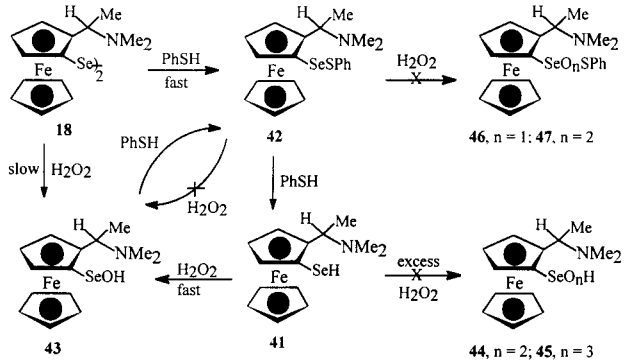

Scheme 6

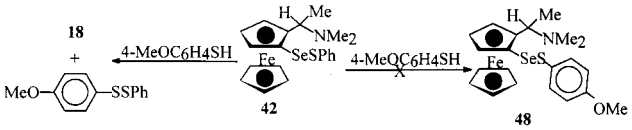

When an equimolar amount of H_2O_2 was added to the reaction mixture containing selenol **41**, two signals at 452.5 and 1174.9 ppm were observed due to the formation of **18** and **43**, respectively. When **18** was treated with PhSH and H_2O_2 simultaneously, two signals were observed at 469.4 and 1174.9 ppm which correspond to the selenenyl sulfide (**42**) and selenenic acid (**43**), respectively. The addition of excess H_2O_2 produced neither the overoxidized acids such as seleninic acid (**44**) and selenonic acid (**45**) nor the overoxidized thiol ester such as seleninic acid thiol ester (**46**) or selenonic acid thiol ester (**47**), thus indicating higher stability of **42** and **43** against further oxidation. The formation of **43** in the presence of H_2O_2 was also confirmed by treating the diselenide **18** with H_2O_2. When **18** was treated with an equimolar amount of H_2O_2, a signal at 1174.9 ppm due to the formation of **43** was observed whereas the signals expected for **44** and **45** were not observed even at higher concentrations of H_2O_2. Similar to the ^{77}Se NMR chemical shift of **36** and the selenenic acid derived from **5**, a large downfield shift in compound **43** indicates a strong Se···N interaction in solution when electron-withdrawing −OH groups are bound to the selenium. When PhSH (1 equiv) was added to the reaction mixture containing **43**, the signal observed at 1174.9 ppm for **43** disappeared completely and a new signal at 468.9 ppm was observed for the selenenyl sulfide, **42**. These reaction sequences are shown in Scheme 5.

Crucially, in contrast to the behavior of **35**, the conversion of the selenenyl sulfide (**42**) to the selenenic acid (**43**) state (reverse GPx cycle) was not observed even at higher concentrations of H_2O_2. This indicates that the nucleophilic attack of PhS^- at sulfur is the favored process in this case. To prove this, two independent experiments were carried out in which the pure **42** was treated separately with H_2O_2 and PhSH under identical experimental conditions. The reaction of **42** with H_2O_2 did not give any signal for **43** whereas with PhSH it produced a new signal at 448.5 ppm which corresponds to the diselenide (**18**). Moreover, when **42** was treated with 4-methoxybenzenethiol, no signal was observed for a new selenenyl sulfide (**48**) but it gave a signal at 448.5 ppm for the diselenide (**18**) (Scheme 6). This strongly suggests that the thiolysis of the selenenyl sulfide takes place at the sulfur rather than the selenium atom.

This was also proved by UV spectroscopy by following the absorbance at 305 nm due to the formation of PhSSPh. When **18** (0.01 mM) was treated with PhSH (0.02 mM), an increase in the absorption was clearly observed. Moreover, the absorption

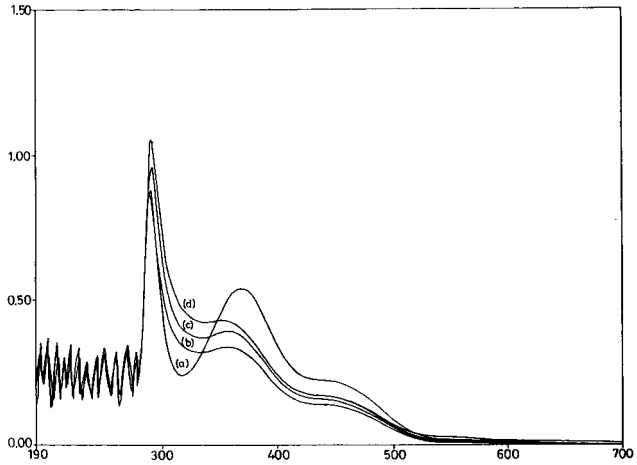

Figure 6. (a) UV spectrum of pure **18** in $CHCl_3$ and (b−d) after gradual addition of PhSH.

Scheme 7

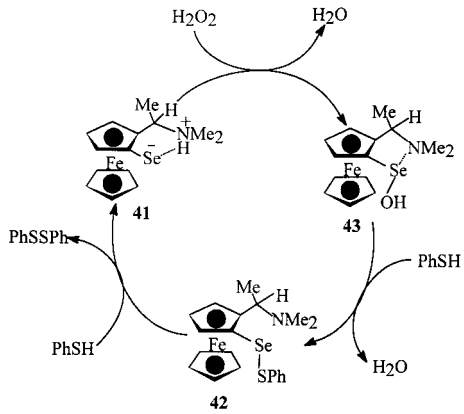

band due to **18** at 370.5 nm disappeared upon PhSH (0.1 mM) addition and a new band appeared at 355.5 nm due to the formation of selenenyl sulfide, **42**. Further addition of PhSH produced PhSSPh as evidenced by a gradual increase in the absorption at 305 nm (Figure 6).

From these experiments it is evident that the reaction of diselenide (**18**) with PhSH produces selenol (**41**) and selenenyl sulfide (**42**). The rapid reaction of **41** with H_2O_2 produces **43**, which in turn reacts rapidly, due to relatively stronger Se···N interaction compared with **42**, with PhSH to produce **42**. Since there is no Se···N interaction in **42**, presumably due to protonation of nitrogen base by thiol, the nucleophilic attack of PhS^- takes place preferentially at sulfur to regenerate **41** and thus complete the catalytic cycle (Scheme 7). It is interesting to note that the peroxidase activity of the semisynthetic enzyme selenosubtilisin could be enhanced by protonating the His64 residue in the selenenyl sulfide (ESeSAr) form.[10] For selenosubtilisin, NMR, crystallographic, and kinetic data all indicate the presence of strong interactions between the deprotonated selenium prosthetic group and the His 64 residue in the selenol (ESeH) and seleninic acid ($ESeO_2H$) species. When the histidine side chain is protonated, the conversion of ESeSAr to ESe^- becomes more rapid.

Reactions of Unsubstituted Diselenides with Thiol and Peroxide. To know the mechanism by which the unsubstituted diaryl diselenides catalyze the reduction of H_2O_2, we have carried out several experiments with PhSeSePh (**14**) and diferrocenyl diselenide (**16**) under identical experimental conditions. The reaction of **14** with PhSH was found to be extremely slow. However, the signal due to PhSeSPh was observed in low

intensity at 521.8 ppm, which is shifted upfield compared with **35**. In contrast to **35**, no signal was observed for PhSeOH or other oxidized products when an excess of H_2O_2 was added to the mixture containing PhSeSPh. When the PhSeSPh was treated with another equivalent of PhSH, the intensity of the signal due to PhSeSPh was reduced with an increase in the intensity of the PhSeSePh signal. The reaction of diselenide with H_2O_2 produced a signal at 1216.6 ppm which can be assigned to the overoxidized selenonic acid, $PhSe(O)_2OH$, owing to the ready disproportionation of benzeneselenenic acid to other oxidized species such as $PhSe(O)_2OH$ and $PhSe(O)_3H$. Since the signal due to seleninic acid, PhSe(O)OH, is known to appear at 1152.0 ppm, the signal at 1216.7 ppm may be ascribed to the selenonic acid. When PhSH (1 equiv) was added to this mixture, a signal at 522.4 ppm was observed for the PhSeSPh. Although the reaction was found to be slow, this clearly indicates that the selenonic acid reacts with PhSH to produce PhSeSPh. The low activity of PhSeSePh can, therefore, be ascribed to the slow reaction of PhSeSPh with thiol and further oxidation of selenenic acid to the overoxidized products due to the absence of basic amino groups. Reactions of compound **16** with PhSH and H_2O_2 were found to be exactly similar to the one observed for **14**. However, the reaction of **16** with PhSH was found to be somewhat faster than that of **14**, which is probably responsible for the slight enhancement in the activity of **16** compared with that of **14**.

Reactions of Other Nitrogen-Containing Diselenides with Thiol and Peroxide. We have also studied the reactions of compounds **3**, **17**, **19**, and **21** with PhSH and H_2O_2. The chemical shift values of the corresponding selenenyl sulfides are 562.3, 460.9, 468.9, and 576.3 ppm, respectively. The addition of 1 equiv of PhSH to the well-known GPx mimic **3** produced two new signals at 6.6 and 562.3 ppm, which correspond to the selenol (**49**) and the selenenyl sulfide (**50**), respectively. In this case the signal due to diselenide **3** (425.7 ppm) disappeared completely. The signal due to **50** (562.1 ppm) is shifted upfield by 13 ppm compared with that of **35**, which indicates that the Se···N interaction in **50** is weaker than that of **35**. A slight decrease in the intensity of signal due to **50** upon H_2O_2 addition indicates a partial conversion of this derivative into selenenic acid **51** (1163.8 ppm). This is consistent with the report of Tomoda et al. where the selenenyl sulfide derived from **5** was partially converted to the corresponding selenenic acid derivative by addition of H_2O_2.

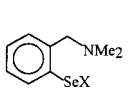

49, X = H; **50**, X = SPh
51, X = OH

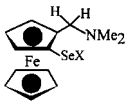

52, X = H; **53**, X = SPh
54, X = OH

Although the structure of **17** is similar to that of **18** and **19**, the NMR behavior of its derivatives was found to be different. While the addition of PhSH produced a signal at 460.9 ppm due to the formation of selenenyl sulfide, **53**, the signal for the selenol (**52**) was not observed even when an excess of PhSH was added. This indicates that the unstable selenol oxidizes to the corresponding diselenide in the presence of air. Addition of H_2O_2 to **17** afforded the selenenic acid **54** (1173.9 ppm), which was found to be unstable and decomposed over a period of time to give an insoluble red precipitate. The instability of selenol and selenenic acid is probably responsible for the low activity of **17** as compared with **18** and **19**.

X-ray Crystallographic Study. The ORTEP diagrams of compounds **12**, **18**, **20**, **21**, and **22** are shown in Figures 7, 8, 9, 10, and 11, respectively. The main feature in these structures is the intramolecular nonbonding interactions between the heteroatom (N or O) and the selenium atoms. In compound **12**, the Se···O distances [Se(1A)···O(1A) = 3.006 Å; Se(1B)···O(1B) = 2.940 Å] are significantly shorter than the sum of the van der Waals radii (3.40 Å). The average Se···O distance (2.973 Å) is considerably longer than the Se···O distance [2.476(3) Å] reported for (phenylseleno)iminoquinone,[27] but much closer to the average Se···O distance (2.977 Å) reported for the diselenide **6** (R = OMe).[28] In addition to the intramolecular Se···O interactions, some intermolecular interactions between selenium atoms were also found in the crystal lattice. The Se···Se intermolecular distance of 3.822 Å is considerably shorter than the van der Waals distance of these two atoms.

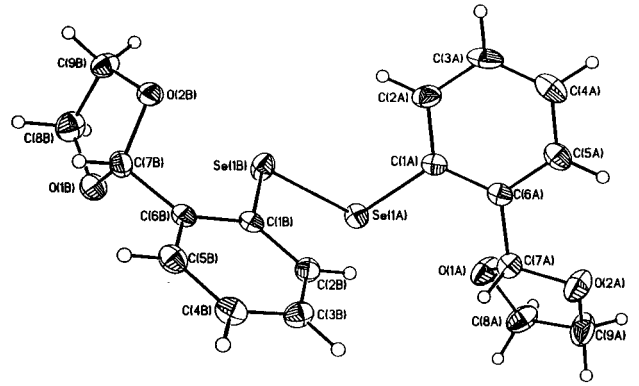

Figure 7. The molecular structure of **12**. Selected bond lengths (Å) and angles (deg): Se(1A)−C(1A) 1.939(5); Se(1A)−Se(1B) 2.3181(7); Se(1B)−C(1B) : 1.936(4); Se(1A)−O(1A) 3.006(1); Se(1B)−O(2B) 2.940(1); C(1A)−Se(1A)−Se(1B) 101.98(13); C(1B)−Se(1B)−Se(1A) 103.28(14); C(2A)−C(1A)−Se(1A) 120.7(4); C(6A)−C(1A)−Se(1A) 119.9(4); C(2B)−C(1B)−Se(1B) 121.4(4); C(6B)−C(1B)−Se(1B) 119.0(3).

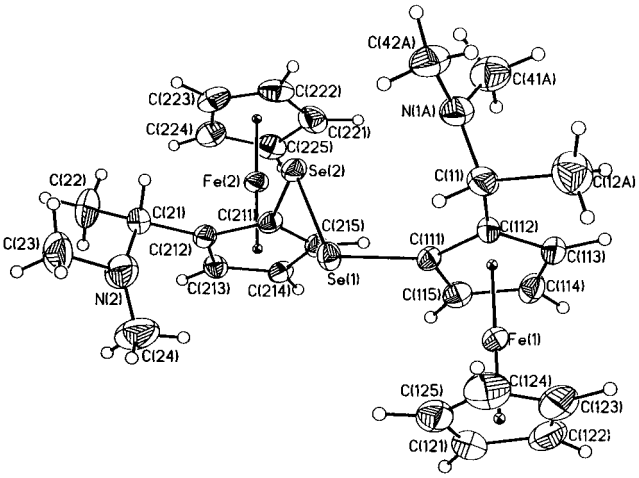

Figure 8. The molecular structure of **18**. Selected bond lengths (Å) and angles (deg): Se(1)−C(111) 1.893(7); Se(1)−Se(2): 2.3487(12) Se(2)−C(211): 1.895(8) Se(2)−N(2) 3.915(5); Se(1)−N(1A) 3.697(5); Se(1)−N(1B) 4.296(5); N(1A)−C(111)−N(1B) 29.31(2); Se(2)−Se(1)−C(111) 100.6(2); Se(1)−Se(2)−C(211) 100.1(2); C(115)−C(111)−Se(1) 124.4(7); C(112)−C(111)−Se(1) 126.9(6); C(215)−C(211)−Se(2) 125.2(6); C(212)−C(211)−Se(2) 127.2(6).

As can be seen from Table 3, the Se···N distances in compounds **18** and **20**−**22** are not identical. In contrast to the other related diselenides based on aryl substrate, compound **18**

(27) Barton, D. H. R.; Hall, M. B.; Lin, Z.; Parekh, S. I.; Reibenspies, J. *J. Am. Chem. Soc.* **1993**, *115*, 5056.
(28) Fragale, G.; Neuburger, M.; Wirth, T. *Chem. Commun.* **1998**, 1867.

Table 3. Comparison of Bond Lengths and Angles of Diselenides **12**, **18**, and **20**−**22**

compd	Se···N distances (Å)	Se−Se distances (Å)	Se−C distances (Å)	C−Se−Se−C dihedral angle (deg)
3	2.856, 2.863	2.357(1)	1.940(4), 1.933(4)	93.8
12	2.940,[a] 3.006[a]	2.3181(7)	1.939(5), 1.936(4)	97.2
18	3.697, 4.296	2.3487(12)	1.893(7), 1.895(8)	−35.46
19	3.980,[b] 4.120[b]	2.347(2)	1.891(1), 1.880(1)	94.10
20	2.705, 2.891	2.3536(8)	1.937(5), 1.946(5)	87.50
21	2.780, 2.798	2.3544(14)	1.946(9), 1.940(9)	−75.72
22	2.628, 2.652	2.383(2)	1.943(12), 1.940(13)	95.63

[a] Se···O distances. [b] Reference 14.

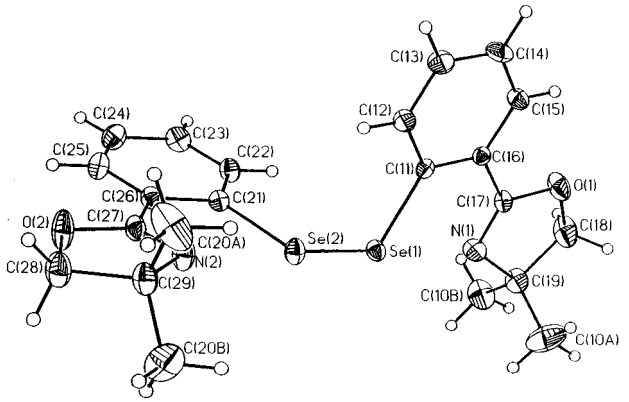

Figure 9. The molecular structure of **20**. Selected bond lengths (Å) and angles (deg): Se(1)−N(1) 2.819(5); Se(2)−N(2) 2.705(5); Se(1)−C(11) 1.937(5); Se(2)−C(21) 1.946(5); O(1)−C(17) 1.356(6); O(1)−C(18) 1.436(7); O(2)−C(27) 1.350(6); O(2)−C(28) 1.452(6); N(1)−C(17) 1.255(6); N(1)−C(19) : 1.486(6); N(2)−C(27) 1.250(6); N(2)−C(29) 1.479(6); Se(1)−Se(2) 2.3536(8); C(12)−C(11)−Se(1) 120.7(4); C(26)−C(21)−Se(2) 119.8(4); C(16)−C(11)−Se(1) 121.2(3); C(11)−Se(1)−Se(2) 102.57(14); C(22)−C(21)−Se(2) 121.4(4); C(21)−Se(2)−Se(1) 101.46(14).

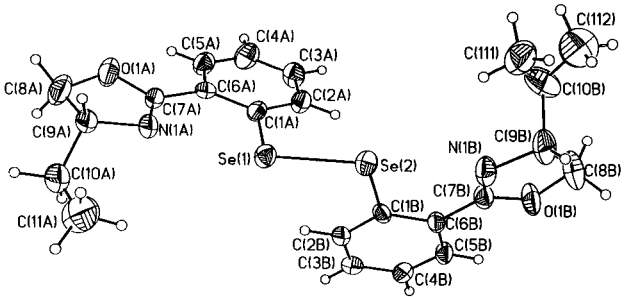

Figure 10. The molecular structure of **21**. Selected bond lengths (Å) and angles (deg): Se(1)−N(1A) 2.798(5); Se(2)−N(1B) 2.780(5); Se(1)−C(1A) 1.946(9); Se(2)−C(1B) 1.940(9); O(1A)−C(7A) 1.370-(11); O(1A)−C(8A) 1.45(2); O(1B)−C(7B) 1.360(11); O(1B)−C(8B) 1.429(14); N(1A)−C(7A) 1.256(12); N(1A)−C(9A) 1.468(11); N(1B)−C(7B) 1.264(13); N(1B)−C(9B) 1.47(2); Se(1)−Se(2) 2.3544(14); C(2A)−C(1A)−Se(1) 120.3(7); C(6B)−C(1B)−Se(2) 119.2(7); C(6A)−C(1A)−Se(1) 120.4(8); C(1A)−Se(1)−Se(2) 102.2(3); C(2B)−C(1B)−Se(2) 122.2(7); C(1B)−Se(2)−Se(1) 102.8(3).

does not have any Se···N intramolecular interactions. As can be seen from the Figure 8, the amino groups are pointed away from the selenium atoms. The Se···N atomic distances of 3.697 [Se(1)···N(1A)], 4.296 [Se(1)···N(1B)], and 4.296 Å [Se(2)···N(2)] for compound **18** are greater than the sum of their van der Waals radii (3.54 Å).[29] The NMe_2 group present in one of the five-membered rings is disordered over two positions. All other bond lengths and angles are normal and are much closer to (*S*,*R*;*S*,*R*)-(−)-bis(2-*N*,*N*-dimethylaminoethyl)ferrocenyl diselenide.[14b] In compound **20**, the atomic distances of Se(1)···N(1) and Se(2)···N(2) are 2.819(5) and 2.705(5) Å, respectively, both of which are larger than the sum of their covalent radii (1.87 Å) but significantly shorter than the sum of the corresponding van der Waals radii (3.5 Å). One of the five-membered rings lies in the plane, whereas for the other ring, there is a twist around the C(26)−C(27) bond such that the nitrogen atom present in this ring is directed slightly away from the selenium atom. The unequal Se···N distances in this compound indicate that the steric effects may play an obvious role.

(29) Pauling L. In *The Nature of the Chemical Bond*, 3rd ed.; Cornell University Press: Ithaca, New York, 1960.

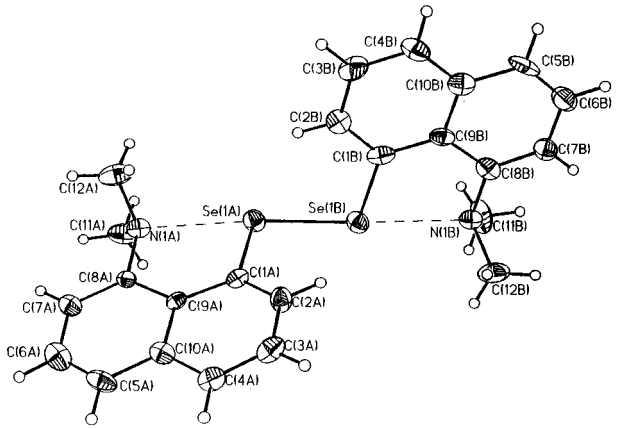

Figure 11. The molecular structure of **22**. Selected bond lengths (Å) and angles (deg): Se(1A)−N(1A) 2.652; Se(1B)−N(1B) 2.628; Se(1A)−C(1A) 1.943(12); Se(1A)−Se(1B) 2.383(2); Se(1B)−C(1B) 1.940(13); C(1B)−Se(1B)−Se(1A) 102.1(4); C(1A)−Se(1A)−Se(1B) 100.6(3); C(9A)−C(1A)−Se(1A) 118.0(8); C(2A)−C(1A)−Se(1A) 122.5(10); C(9B)−C(1B)−Se(1B) 121.6(10); C(2B)−C(1B)−Se(1B) 121.1(11); Se(1A)−N(1A)−C(1A) 76.8; C(7B)−C(8B)−N(1B) 122.4(14); Se(1B)−N(1B)−C(1B) 76.1; Se(1A)−N(1A)−Se(1B) 175.3; Se(1B)−N(1B)−Se(1A) 177.8.

Compound **21** crystallizes in an orthorhombic system with 4 molecules per unit cell. The coordination geometry around the selenium is similar to that of **20**. Atomic distances of Se(1)···N(1A) and Se(2)···N(1B) are 2.798(5) and 2.780(5) Å, respectively, both of which are almost equal to the values observed for **20**. However, in contrast to the values observed for **20**, the two Se···N distances are equal. Other bond lengths and angles are almost equal to the corresponding values observed for compound **20**. The methyl group attached to C(10B) is disordered over two positions [C(111) and C(112)]. The absolute configurations around both chiral carbon centers, C(9A) and C(9B), were found to be "R". The crystal structure of compound **22** involves packing of four discrete molecules in the unit cell. The Se···N distances Se(1A)···N(1A) [2.652(2) Å] and Se(1B)···N(1B) [2.628(2) Å] are much shorter than that of **3** and **18**−**22**. In the case of **22**, the C(1A)−Se(1A)−Se(1B)−C(1B) torsion angle is 95.63° and thus has a transoid conformation. The most interesting feature of the structure is that the compound has crystallized in a chiral space group $P2_12_12_1$. The chirality of the compound may arise due to the strong Se···N

interaction that can twist the whole molecule in such a way that it becomes chiral. In all the diselenides, the Se−Se and C−Se distances relate well to the corresponding distances reported for other diselenides which range from 2.29 to 2.39 Å. These distances are also close to that reported for **3**[12b] and **19**.[14b] Refinement of the Flack enantiopole parameter[30] for the chiral compounds **18**, **20**, and **22** led to a value of ∼0, thus confirming the enantiomeric purity of the crystals.

Conclusion

From this study, we conclude that the diselenides (**18**, **19**) derived from *N*,*N*-dimethylaminoethylferrocene catalyze the reduction of H_2O_2 with thiol more efficiently than the oxazoline based diselenides (**20**, **21**) and Wilson's catalyst (**3**). The thiol peroxidase activities of these compounds depend on the strength of Se···N nonbonded interactions in the intermediates produced during the catalytic process. In the more active compounds, the basic nitrogen is involved in a stabilizing interaction in the selenol and selenenic acid derivatives, whereas in the less active compounds, the nitrogen atom interacts with selenium in all three intermediates, viz., selenol, selenenic acid, and selenenyl sulfide states. *The reactivity of selenenyl sulfide toward the thiol, therefore, determines the peroxidase activity of the compounds.* The basic nitrogen atom in model compounds should, therefore, be positioned in such a way that it (i) abstracts H^+ from RSeH and activates the selenol into reactive selenolate anion (RSe^-), (ii) interacts strongly with selenium in RSeOH to increase the stability of this species against further oxidation and to increase the nucleophilic attack of thiol at selenium, and (iii) deprotonates the thiol sulfhydryl group to provide a high local concentration of nucleophilic thiolate anion. The studies presented here will undoubtedly enhance our understanding of the mechanism of model compounds and may ultimately yield insights that result in improved GPx mimics.

Experimental Section

General Procedures. All reactions were carried out under nitrogen or argon with standard vacuum-line techniques. Solvents were purified by standard procedures[31] and were freshly distilled prior to use. Melting points were recorded in capillary tubes and are uncorrected. IR spectra were recorded on a Bio-Rod FT-IR spectrometer model FTS165. ^1H and ^{13}C NMR spectra were obtained at 300 and 75.42, respectively, in $CDCl_3$ on a Varian VXR 300S spectrometer. ^1H and ^{13}C chemical shifts are cited with respect to $SiMe_4$ as internal standard. Elemental analyses were performed on a Carlo-Erba model 1106 elemental analyzer. Mass spectra were recorded at room temperature on a JEOL D-300 (EI/CI) mass spectrometer. In the case of isotopic patterns, the value given is for the most intense peak.

Synthesis of bis[*o*-formylphenyl] diselenide acetal (12): To a solution of *o*-bromobenzaldehyde acetal (**24**)[12c] (5.18 g, 22.61 mmol) in dry ether (100 mL) was added dropwise a 1.6 M solution of n-BuLi (15.38 mL, 24.61 mmol) at room temperature over a period of 5 min. The mixture was stirred for additional 5 min to get a cloudy white slurry. Selenium powder (1.78 g, 22.54 mmol) was added slowly with vigorous stirring. After refluxing for 30 min, the solution was cooled and poured into ice water (500 mL). The resulting organic layer and the dichloromethane extracts (3 × 20 mL) from the aqueous layer were combined, washed with water, dried over anhydrous sodium sulfate, and concentrated to 10 mL. A light yellow solid, which precipitated out from the resulting solution on keeping 15 days in the refrigerator (4 °C), was filtered and dried under nitrogen. Yield 1.03 g (20%); mp 108−110 °C; IR (KBr) 3058, 2953, 2886, 1587, 1466, 1392, 1213, 1088 cm^{-1}; ^1H NMR ($CDCl_3$) δ 7.81−6.01 (m, 8H), 6.01 (s, 2H), 4.02−4.21 (m, 8H); ^{13}C NMR ($CDCl_3$) δ 136.66, 132.38, 130.52, 130.11, 127.06, 126.92, 103.40, 65.25; ^{77}Se NMR ($CDCl_3$) δ 408.4; *m*/*z* 456 (M^+), 307, 289, 227, 154 (100), 136. Anal. Calcd for $C_{18}H_{18}O_4Se_2$: C, 47.39; H, 3.98. Found: C, 47.66; H, 3.99.

Synthesis of bis[2,5-dimethyl-4-*tert*-butylphenyl]diselenide (13): A 100-mL three-necked flask was equipped with a magnetic stirrer, a pressure equalizing dropping funnel, and reflex condenser mounted with nitrogen source. To the flask were added 2-bromo-5-*tert*-butyl-*m*-xylene (**26**)[16] (2.42 g, 10.03 mmol), magnesium (0.24 g, 10.03 mmol), and ether (10 mL). The reaction was initiated by the addition of iodine. The reaction mixture was heated at reflux for 1 h, then dry THF (25 mL) was added. This reflux was continued for an additional 4 h to get a white slurry of **27**. While a slow stream of nitrogen was passed through the nitrogen inlet, Se powder (0.79 g, 10.01 mmol) was added. The reflux was continued until all the selenium had reacted to give a red solution. The resulting solution was poured into a beaker and oxygen was bubbled for 15 min. After the complete evaporation of THF, the red solid was dissolved in dichloromethane, filtered through Celite, and dried over sodium sulfate. Evaporation of the solvent afforded an orange solid that was recrystallized from hexane to give needle-shaped crystals. Yield 2.05 g (85%); mp 120−122 °C; IR (KBr) 2964, 1644, 1592, 1433, 1229, 1073 cm^{-1}; ^1H NMR ($CDCl_3$) δ 1.20 (s, 18H), 2.23 (s, 12H), 7.01 (s, 4H); ^{13}C NMR ($CDCl_3$) δ 152.41, 143.32, 128.72, 124.49, 34.35, 31.24, 24.38; ^{77}Se NMR ($CDCl_3$) δ 369.3. Anal. Calcd for $C_{24}H_{34}Se_2$: C, 60.00; H, 7.13. Found: C, 59.94; H, 7.11.

Synthesis of dinaphthyl diselenide (15): In a 100-mL three-necked flask magnesium (0.36 g, 14.81 mmol) was taken up in 25 mL of anhydrous THF. 1-Bromonaphthlene (3.11 g, 15.02 mmol) was added dropwise with constant stirring under reflux conditions. The stirring was continued until the completion of the reaction as indicated by the disappearance of magnesium. Selenium powder (1.25 g, 15.83 mmol) was added to the reaction mixture in portions over a period of 30 min so as to maintain a gentle reflux. After 2 h of reflux, the solution was poured into a beaker which was kept open overnight for aerial oxidation. The product was extracted with ether (2 × 25 mL). The ether solution was washed with water and the organic layer was separated, dried over sodium sulfate, and evaporated under vacuum to give an yellow crystalline solid. Yield 1.13 g (36.6%); mp 76−78 °C dec. Anal. Calcd for $C_{20}H_{14}Se_2$: C, 58.27; H, 3.42. Found: C, 58.24; H, 3.21. All other data are in accordance with the literature values.[32]

Synthesis of diferrocenyl diselenide (16): Compound **16** was synthesized by following the literature method with slight modifications.[17] A stirred solution of ferrocene (2.24 g, 12.04 mmol) in dry THF (10 mL) was treated dropwise with a 1.6 M solution of t-BuLi in pentane (6.26 mL, 10.02 mmol) via a syringe at 0 °C. After being stirred for 30 min at this temperature, the solution was warmed to room temperature. Selenium powder (0.79 g, 10.01 mmol) was added under a brisk flow of N_2 gas and stirring was continued for 1 h. The reaction mixture was then poured into a beaker and oxygen was passed at a moderate rate for half an hour. The compound was extracted with 3 × 20 mL of CH_2Cl_2 and filtered. The filtrate was evaporated to dryness to give a brown solid. The crude product was chromatographed on a silica gel column. The unreacted ferrocene was eluted with hexane and the diferrocenyl diselenide was eluted with a 3:1 hexane:CH_2Cl_2 mixture. Slow evaporation of the CH_2Cl_2 solution gave red crystals of the desired compound. Yield 1.58 g (50%); mp 184−186 °C (lit.[17] mp 185−187 °C); ^{77}Se NMR ($CDCl_3$) δ 479.2. Anal. Calcd for $C_{20}H_{18}Fe_2Se_2$: C, 45.49; H, 3.44. Found: C, 5.58; H, 3.42. ^1H and ^{13}C NMR data are consistent with the values reported in the literature.[17]

Synthesis of bis[2-(*N*,*N*-dimethylaminomethyl)ferrocenyl]diselenide (17): Compound **17** was synthesized by following the literature method with minor modifications.[18] A stirred solution of *N*,*N*-dimethylaminomethylferrocene (2.45 g, 10.08 mmol) in dry ether (10 mL) was treated dropwise with a 1.6 M solution of n-BuLi in hexane (6.30 mL, 10.08 mmol) via a syringe at room temperature. After the solution was stirred for 24 h at this temperature, selenium powder (0.79 g, 10.01 mmol) was added under a brisk flow of N_2 gas and stirring was continued for 5 h. The reaction mixture was then poured into a beaker

(30) Flack, H. *Acta Crystallogr. Sect. A* **1983**, *39*, 876.

(31) Perrin, D. D.; Armarego, W. L. F.; Perrin, D. R. *Purification of Laboratory Chemicals*, 2nd ed.; Pergamon: Oxford, 1980.

(32) Bhasin, K. K.; Gupta, V.; Gupta, S. K.; Sanan, K.; Sharma, R. P. *Ind. J. Chem*. **1994**, *33A*, 1110.

and oxygen was passed at a moderate rate for 1 h. The solution was filtered, dried, and evaporated to give a brown oil. The crude product was chromatographed on a silica gel column. The unreacted ferrocene was eluted with hexane and **17** was eluted with a 2:1 hexane:CH_2Cl_2 mixture. Slow evaporation of the CH_2Cl_2 solution gave red crystals of the desired compound. Yield 0.65 g (20%); mp 122−124 °C (lit.[18] mp 126 °C); ^{77}Se NMR ($CDCl_3$) δ 576.7. Anal. Calcd for $C_{26}H_{32}Fe_2N_2Se_2$: C, 48.63; H, 5.02; N, 4.36. Found: C, 48.62; H, 5.13; N, 4.25. ^{1}H and ^{13}C NMR data are in accordance with the literature values.[18]

Synthesis of bis[2-(4,4-dimethyl-2-oxazolinyl)phenyl]diselenide (20): A stirred solution of 4,4-dimethyl-2-phenyloxazoline, (1.78 g, 10.16 mmol) in dry hexane (75 mL) was treated dropwise with a 1.6 M solution of n-BuLi in hexane (6.88 mL, 11.01 mmol) via syringe under N_2 at 0 °C. On stirring for 1 h at room temperature the white precipitate of the lithiated product was obtained. The solvent was removed by syringe and 50 mL of dry ether was added. The solution was cooled to 0 °C, selenium powder (0.79, 10.01 mmol) was added, and stirring was continued for an additional 2 h at 0 °C. The reaction mixture was then removed from the N_2 line and poured into a beaker containing cold aqueous $NaHCO_3$, and O_2 was passed at a moderate rate for 15 min. The organic phase was separated, dried over Na_2SO_4, and filtered. The filtrate was evaporated to dryness to give a yellow oil. The crystalline solid of the desired compound (**20**) was obtained upon cooling. The compound was recrystallized from a chloroform/methanol mixture to give pale yellow crystals. Yield 1.54 g (60%); mp 158−160 °C; IR (KBr) 2935, 1649, 1561, 1468, 1433, 1386, 1319, 1188, 1075 cm^{-1}; ^{1}H NMR ($CDCl_3$) δ 1.42 (s, 12H), 4.10 (s, 4H), 7.26−7.48 (m, 4H), 7.92−7.95 (m,4H); ^{13}C NMR ($CDCl_3$) δ 28.97 (s), 68.86 (s), 79.26 (s), 161.75 (s), 125.88 (s), 126.79 (s), 129.59 (s), 130.85 (s), 131.48 (s), 133.91 (s); ^{77}Se NMR ($CDCl_3$) δ 454.7; *m*/*z* 506 (M^+), 426, 299, 253 (100), 199, 181, 110, 77, 54. Anal. Calcd for $C_{22}H_{24}N_2O_2Se_2$: C, 52.18; H, 4.78; N, 5.53. Found: C, 52.52; H, 4.86; N, 5.58.

Synthesis of bis[2-(4-ethyl-2-oxazolinyl)phenyl]diselenide (21): A stirred solution of 4-*R*-(−)-ethyl-2-phenyloxazoline (1.78 g, 10.16 mmol) in dry ether (75 mL) was treated dropwise with a 1.6 M solution of n-BuLi in hexane (6.88 mL, 11.01 mmol) via syringe under N_2 at 0 °C. On stirring the reaction mixture for 5 h at this temperature the lithiated product was obtained. Selenium powder (0.79 g, 10.01 mmol) was added to the solution under a brisk flow of N_2 gas and stirring was continued for an additional 2 h at 0 °C. The reaction mixture was then removed from the N_2 line and poured into a beaker containing cold aqueous $NaHCO_3$ and O_2 was passed at a moderate rate for 15 min. The organic phase was separated, dried over Na_2SO_4, and filtered. The filtrate was evaporated to dryness to give a yellow oil. The crystalline solid of the desired compound was obtained upon cooling. The compound was recrystallized from the chloroform/methanol mixture to give pale yellow crystals. Yield 1.03 g (40%); mp 120−122 °C; IR (KBr) 2962, 1645, 1464, 1430, 1359, 1135, 1069 cm^{-1}; . $[\alpha]^{23}_D$ 113.9 (*c* 1, $CHCl_3$); ^{1}H NMR ($CDCl_3$) δ 1.10 (t, 6H), 1.68 (m, 4H), 4.08 (t, 2H), 4.40 (m, 2H), 4.44 (t, 2H), 7.19−7.27 (m, 4H), 7.79−7.68 (m, 4H); ^{13}C NMR ($CDCl_3$) δ 10.54 (s), 29.16 (s), 68.53 (s), 72.24 (s), 125.64 (s), 126.13 (s), 129.53 (s), 130.52 (s), 131.36 (s), 133.52 (s), 162.98 (s); ^{77}Se NMR ($CDCl_3$) δ 456.56; *m*/*z* 506 (M^+), 427, 253 (100), 199, 181, 103, 70, 54. Anal. Calcd for $C_{22}H_{24}N_2O_2Se_2$: C, 52.18; H, 4.78; N, 5.53. Found: C, 51.92; H, 4.84; N, 5.25

Synthesis of bis[8-(dimethylamino)-1-naphthyl]diselenide (22): A stirred solution of 1-dimethylaminonaphthalene (1.04 g, 6.07 mmol) in dry ether (50 mL) was treated dropwise with a 1.6 M solution of n-BuLi in hexane (4.06 mL, 6.50 mmol) via syringe under N_2 at room temperature. The mixture was stirred for 24 h, during which a yellow precipitate of 8-(dimethylamino)-1-naphthyllithium etherate was slowly formed. To this suspension elemental selenium (0.48 g., 6.08 mmol) was added rapidly. After 3 h all the selenium was consumed to produce a yellow solution of lithium naphthylselenolate. This was poured into a beaker containing aqueous $NaHCO_3$. The resulting organic layer and ethyl acetate extract from the aqueous layer were combined, dried over Na_2SO_4, and concentrated under vacuuo to give a yellow powder. Recrystallization of this from pentane gave yellow crystals. Yield 0.91 g (60%); mp 136−138 °C dec; IR (KBr) 3061, 2979, 2935, 1560, 1447, 1357, 1290, 1207, 1025 cm^{-1}; ^{1}H NMR ($CDCl_3$) δ 2.85 (s, 12H), 7.21 (t, 1H), 7.45 (d, 1H), 7.48 (t, 1H), 7.63 (dd, 1H), 7.7 (dd, 1H), 7.86 (dd, 1H); ^{13}C NMR ($CDCl_3$) δ 46.59, 119.5, 125.79, 125.88, 126.24, 126.9, 128.1, 130.52, 135.98, 151.0; ^{77}Se NMR ($CDCl_3$) δ 485.2, 648.6; *m*/*z* 498 (M^+), 494 (M^+ − 4), 294 (100), 234, 219, 170, 155, 140. Anal. Calcd for $C_{24}H_{24}N_2Se_2$: C, 57.84; H, 4.85; N, 5.62. Found: C, 57.62; H, 4.63; N, 5.85.

Table 4. Crystal Data and Structure Refinement for **12**, **18**, and **20**

	12	**18**	**20**
empirical formula	$C_{18}H_{18}O_4Se_2$	$C_{28}H_{36}N_2Se_2$	$C_{22}H_{24}N_2O_2Se_2$
fw	456.24	670.21	506.35
crystal system	monoclinic	orthorhombic	rhombohedral
space group	$P2_1/c$	$P2_12_12_1$	$R\bar{3}$
a (Å)	8.9690(7)	10.7903(11)	33.198(4)
b (Å)	12.5676(9)	15.1341(12)	33.198(4)
c (Å)	15.6444(12)	17.7815(14)	10.564(2)
α (deg)	90	90	90
β (deg)	95.293(6)	90	90
γ (deg)	90	90	120
V (Å^3)	1755.9(2)	2903.7(4)	10083(2)
Z	4	4	18
D(calcd) (Mg/m^3)	1.726	1.533	1.501
abs coeff (mm^{-1})	4.230	3.524	3.319
obsd reflens [$I > 2\sigma$]	3436	4597	4884
final $R(F)$ [$I > 2\sigma(I)$][a]	0.0455	0.0511	0.0500
$wR(F^2)$ indices [$I > 2\sigma(I)$]	0.0886	0.0870	0.0837
data/restrains/parameters	3436/0/236	4595/15/407	4882/0/281
absolute structure parameter		−0.02(2)	
goodness of fit on F^2	1.018	1.054	1.030

[a] Definitions: $R(F_o) = \sum||F_o| - |F_c||/\sum|F_o|$ and $wR(F_o^2) = \{\sum[w(F_o^2 - F_c^2)^2]/\sum[w(F_c^2)^2]\}^{1/2}$.

Synthesis of 2-[4,4-dimethyl-2-oxazolinyl]phenyl selenol (34): Sodium borohydride (0.08 g, 0.2 mmol) was added to a solution of **20** (50.63 mg, 0.1 mmol) in 1 mL of methanol, and the mixture was allowed to stand for 1 h with occasional shaking. To this was added $CDCl_3$ (2 mL) and the ^{77}Se NMR spectrum of the sample was obtained, showing a resonance at 17.9 ppm, attributed to the borane complex of **34**. The addition of dilute HCl produced a new doublet centered at 9.9 ppm assigned to the air-sensitive selenol, **34**, which was not further characterized. (J_{Se-H} = 20.3 Hz).

Synthesis of [2-(4,4-dimethyl-2-oxazolinyl)phenyl]selenenylphenyl sulfide (35): The diselenide (**20**, 0.51 g, 1.01 mmol) was dissolved in CH_2Cl_2 under air and benzenethiol (0.21 mL, 2.02 mmol) was added to the solution. After 2 h of stirring under air, the reaction mixture was concentrated under reduced pressure. Addition of hexane afforded a white solid that was filtered and dried under nitrogen to give pure **35**. Yield 0.67 g (92%); IR (KBr) 3062, 2965, 2891, 1657, 1560, 1466, 1361, 1282, 1188, 1040 cm^{-1}; ^{1}H NMR ($CDCl_3$) δ 1.44 (s, 6H), 4.14 (s, 2H), 7.10−7.30 (m, 4H), 7.37−7.42 (t, 1H), 7.46−7.50 (d, 2H), 7.80−7.82 (d, 1H), 8.14−8.17 (d, 1H); ^{13}C NMR ($CDCl_3$) δ 161.90, 137.04, 137.01, 131.36, 129.21, 128.86, 127.57, 126.21, 125.76, 125.38, 79.49, 68.46, 28.76; ^{77}Se NMR ($CDCl_3$) δ 576.7; *m*/*z* (FAB) 364 (M^+), 254 (100%), 199, 182, 154, 136. Anal. Calcd for $C_{17}H_{17}NOSSe$: C, 56.35; H, 4.73; N, 3.87. Found: C, 56.30; H, 4.72; N, 3.79.

Kinetic Analysis. The reactions of model compounds with benzenethiol (PhSH) and H_2O_2 were studied in methanol by following the appearance of the disulfide absorption at 305 nm, at 25 °C. Each initial velocity was measured at least 6 times and calculated from the first 5−10% of the reaction. For the peroxidase activity, the rates were corrected for the background reaction between H_2O_2 and PhSH. The actual concentration of PhSH in the kinetic apparatus was measured from the 305 nm absorbance, and rates were corrected for any variation in the concentration of PhSH. The molar extinction coefficient of PhSSPh ($\epsilon_1 = 1.24 \times 10^3$ M^{-1} cm^{-1}) at the wavelength was much larger than that of PhSH ($\epsilon_2 = 9$ M^{-1} cm^{-1}).[7b] The concentration of PhSH (*C*) was therefore calculated from the absorbance (*a*) according to the following equation: $C = (\epsilon_1 C_0 - 2a)/(\epsilon_1 - 2\epsilon_2) \approx C_0 - 2a/\epsilon_1$. The initial reduction rate of H_2O_2 (v_0) was then determined by $1/v$ vs 1/[PhSH] plots using the Grapher program. The concentration of the

Table 5. Crystal Data and Structure Refinement for **21** and **22**

	21	**22**
empirical formula	$C_{22}H_{24}N_2O_2Se_2$	$C_{24}H_{24}N_2Se_2$
fw	506.35	498.37
crystal system	orthorhombic	orthorhombic
space group	$P2_12_12_1$	$P2_12_12_1$
a (Å)	8.778(3)	7.6738(10)
b (Å)	12.643(3)	11.0274(11)
c (Å)	20.268(4)	26.127(3)
α (deg)	90	90
β (deg)	90	90
γ (deg)	90	90
V (Å^3)	2249.2(11)	2210.9(4)
Z	4	4
D(calcd) (Mg/m^3)	1.495	1.497
abs coeff (mm^{-1})	3.306	3.356
obsd reflens [$I > 2\sigma$]	2167	2839
final $R(F)$ [$I > 2\sigma(I)$][a]	0.0456	0.0564
$wR(F^2)$ indices [$I > 2\sigma(I)$]	0.0869	0.1015
data/restrains/parameters	2167/3/276	2831/0/282
absolute structure parameter	0.00(3)	0.03(4)
goodness of fit on F^2	1.061	1.033

[a] Definitions: $R(F_o) = \sum||F_o| - |F_c||/\sum|F_o|$ and $wR(F_o^2) = \{\sum[w(F_o^2 - F_c^2)^2]/\sum[w(F_c^2)^2]\}^{1/2}$.

H_2O_2 stock was determined by permanganate titration. To investigate the dependency of rate on substrate concentrations, the reaction rates were determined at several concentrations of one substrate while keeping the concentration of the other constant. The Lineweaver−Burk plots were obtained using the Grapher 1.09 version, 2D-Graphing System for windows program.[33] For each set of experiments the straight line was drawn by choosing the best fit method.

^{77}Se NMR Analysis. Unless the particular conditions were specified in the text, ^{77}Se NMR spectra were obtained at 95.35 MHz on a Bruker 500 spectrometer under normal atmosphere. The ^{77}Se NMR spectra were recorded using diphenyl diselenide as an external standard. Chemical shifts are reported relative to dimethyl selenide (0 ppm) by assuming that the resonance of the standard is at 461.0 ppm.[6a] All experiments were carried out in 0.1 mmol scale by using a 1:1 mixture of $CDCl_3$ (0.75 mL) and CH_3OH (0.75 mL) as NMR solvent.

(33) Schmitz, D.; Smith, D.; Wall, W. Grapher 1.09, 2-D Graphical system, Golden Software, Inc., 1993.

X-ray Crystallography. The X-ray diffraction measurements for compounds **12**, **18**, **20**, **21**, and **22** were performed at room temperature (295 K) on a Siemens R3m/V diffractometer using graphite-monochromated Mo Kα radiation (λ = 0.71073 Å). The unit cell was determined from 25 randomly selected reflections using the automatic search index and least-squares routine. The data were corrected for Lorentz, polarization, and absorption effects. The structures were solved by routine heavy-atom (using SHELXS 86[34]) and Fourier methods and refined by full-matrix least squares with the non-hydrogen atoms anisotropic and hydrogens with fixed isotropic thermal parameters of 0.07 Å^2 using the SHELXL 93 program.[35] The hydrogens were partially located from difference electron-density maps and the rest were fixed at calculated positions. Scattering factors were from common sources.[36] Some details of data collection and refinement are given in Tables 4 and 5.

Acknowledgment. We are grateful to the Royal Society of Chemistry, London, and the Department of Science and Technology (DST), New Delhi, for funding this work. Additional help from the Regional Sophisticated Instrumentation Centre (RSIC), Indian Institute of Technology (IIT), Bombay, for 300 MHz and Tata Institute of Fundamental Research (TIFR), Bombay, for 500 MHz NMR spectroscopy is gratefully acknowledged. R.J.B. wishes to acknowledge the DoD-ONR program for funds to upgrade the diffractometer.

Supporting Information Available: The details of kinetic and ^{77}Se NMR measurements, tables giving crystal data and details of the structure determination, final atomic coordinates, bond lengths and angles, anisotropic displacement parameters, and hydrogen atom coordinates for **12**, **18**, **20**, **21** and **22** (PDF) as well as CIF data for **12**, **18**, **20**, **21**, and **22**. This material is available free of charge via the Internet at http://pubs.acs.org.

JA994467P

(34) Sheldrick, G. M. Crystallographic Computing 3, Oxford University Press: Oxford, 1985.

(35) Sheldrick, G. M. SHELX 93, Program for Crystal Structure Determination, University of Gottingen, 1993.

(36) *International Tables for X-ray Crystallography*; Kynoch Press: Birmingham, 1974; Vol. 4, pp 99and 149.